Physics of the edge plasma and first wall in fusion devices: Synergistic effects

S. I. Krasheninnikov

University of California San Diego, La Jolla, USA

MEPhI, Moscow, Russia

Introduction

- Magnetic fusion has two major issues: core plasma confinement and the performance of the edge plasma and the first wall
- In many studies edge plasma and the first wall processes are treated separately from each other (e.g. wall physics is studied into depth on linear devices)
- Such separate study of edge plasma and the first wall processes, legitimate in many cases, fails when synergistic effects in edge plasma-first wall interactions become important
- At this moment there is rather long list of experimental data clearly demonstrating synergistic effects in plasma-wall interactions in magnetic fusion devices:

Introduction (con-ed)

- Wall heating in long pulse discharges in JT-60 cause intensive gas desorption from the wall, which triggers MARFE formation (Nakano, 2006)

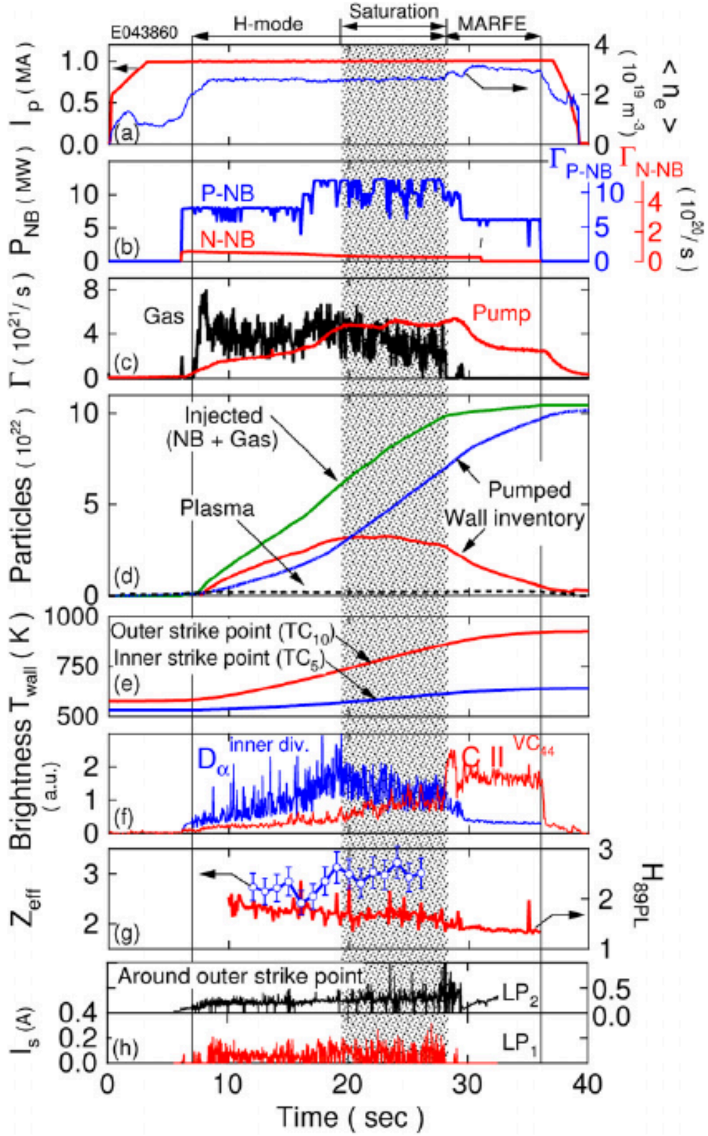

Introduction (con-ed)

- Simplified theoretical models of coupled plasma-wall interactions also predict the possibility of development of thermal instability (Krasheninnikov, 2006)

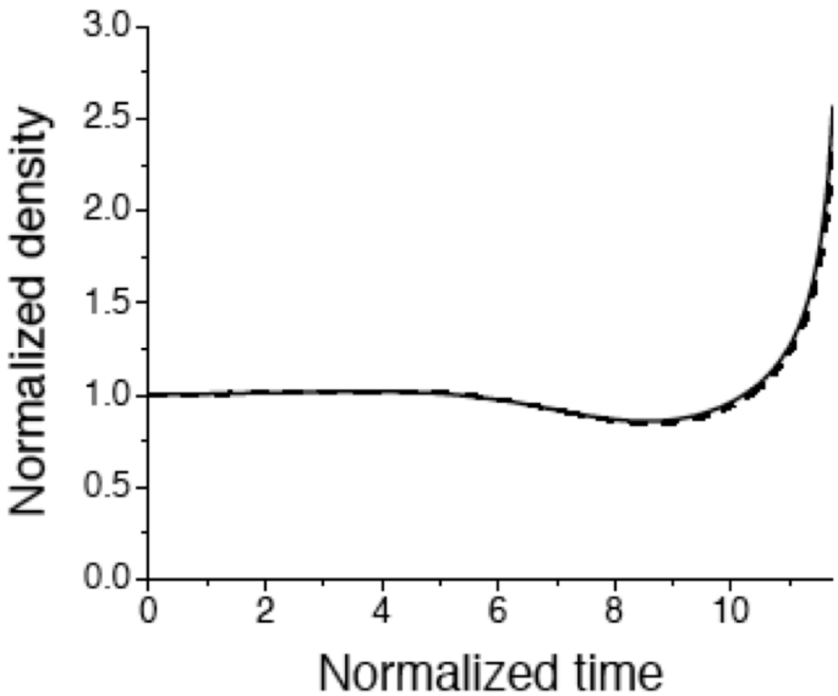

Introduction (con-ed)

- Formation of “hot spots” which eject into plasma large amount of hydrogenic species, impurities, and dust particles which can significantly restrict operational domain or even terminate the discharge (Pégourié, 2009)

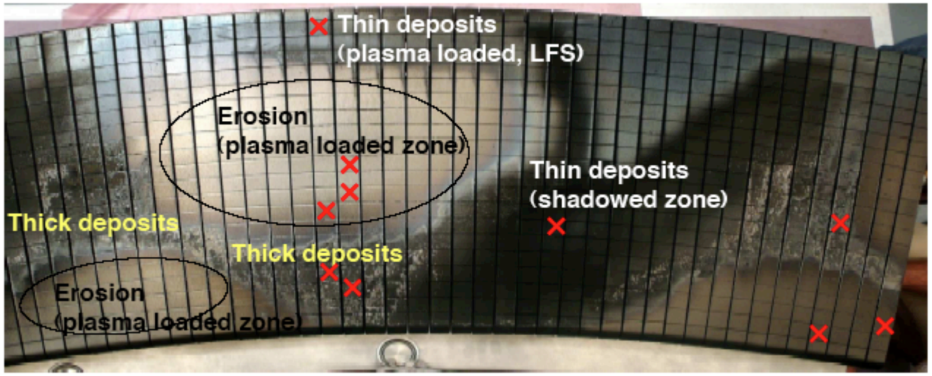

Fig 3a : sector Q6A of the Tore Supra limiter, extracted after the DITS campaign. The different zones of interest are indicated as well as the analysed tiles (crosses)

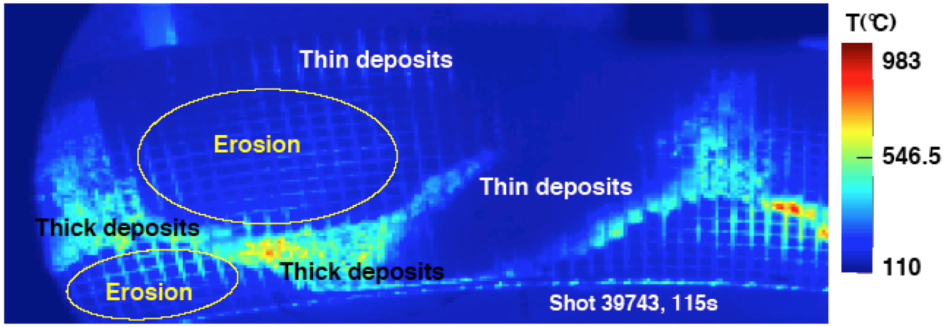

Fig 3b : IR imaging of the limiter sector during the DITS campaign. The different zones of interest are indicated

Introduction (con-ed)

- Recovery of plasma density pedestal after large type-I ELM crash is determined, largely, by the wall outgassing processes since recovery of a good confinement occurs at much shorter time scale (Pigarov, 2014)

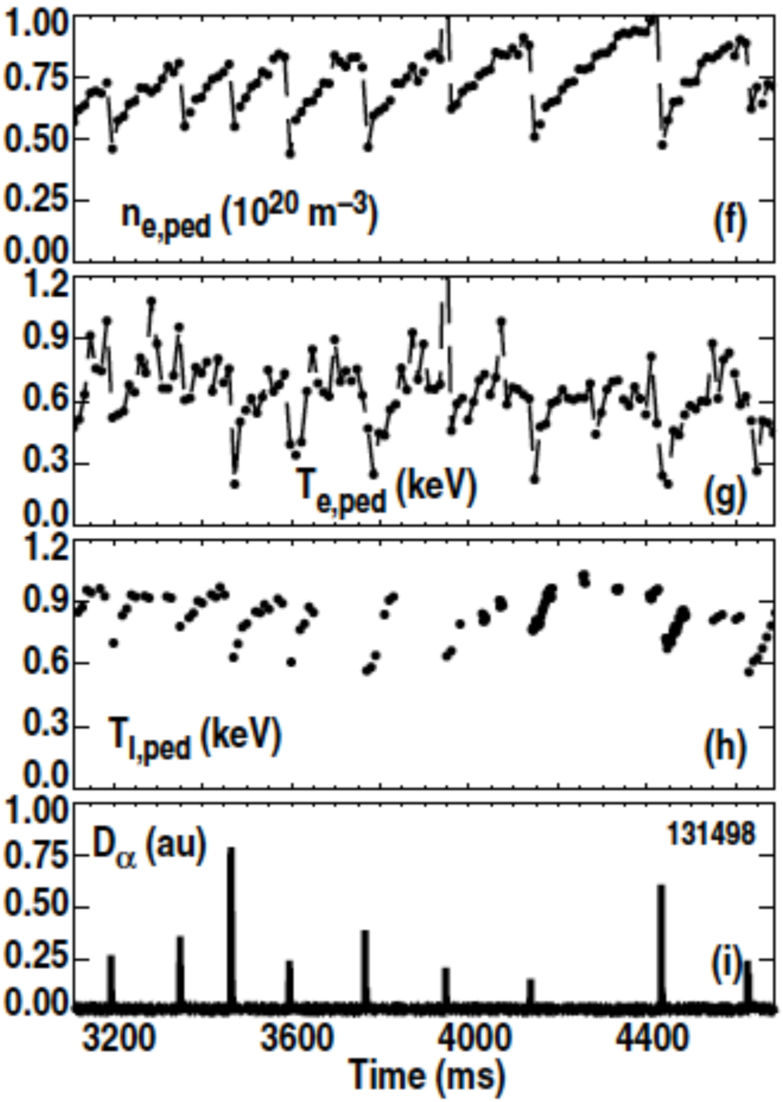

Groebner, 2010

Introduction (con-ed)

- Simulations of ELM-first wall interactions with plasma gun MK-200 show that due to shielding effects of target vapor, only relatively small part (~25%) of large loaded energy comes to the target (Safronov, 2009)

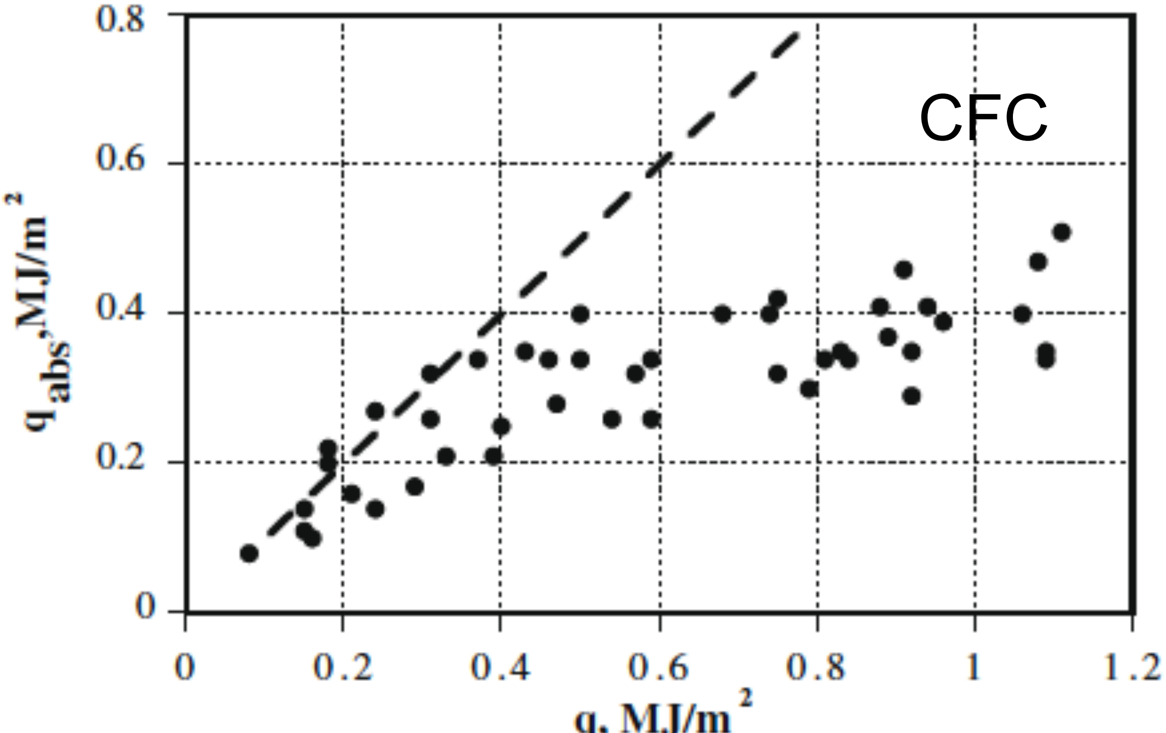

Introduction (con-ed)

- The most complex issues in all considered examples are:
  - Transport of hydrogen in first wall material, and
  - Line radiation transport in opaque plasmas

Outline

- Introduction to hydrogen transport in first wall material
- Introduction to radiation transport in opaque plasmas
- Studies of synergistic effects in edge plasma-first wall interactions:
  - Dynamic edge plasma-wall interactions during ELMs
  - Some issues in shielding effects
  - Effects of secondary electron emission on plasma heat flux
- Conclusions

Hydrogen transport

- Plasma-material interactions (PMI) in our theoretical “dreams”

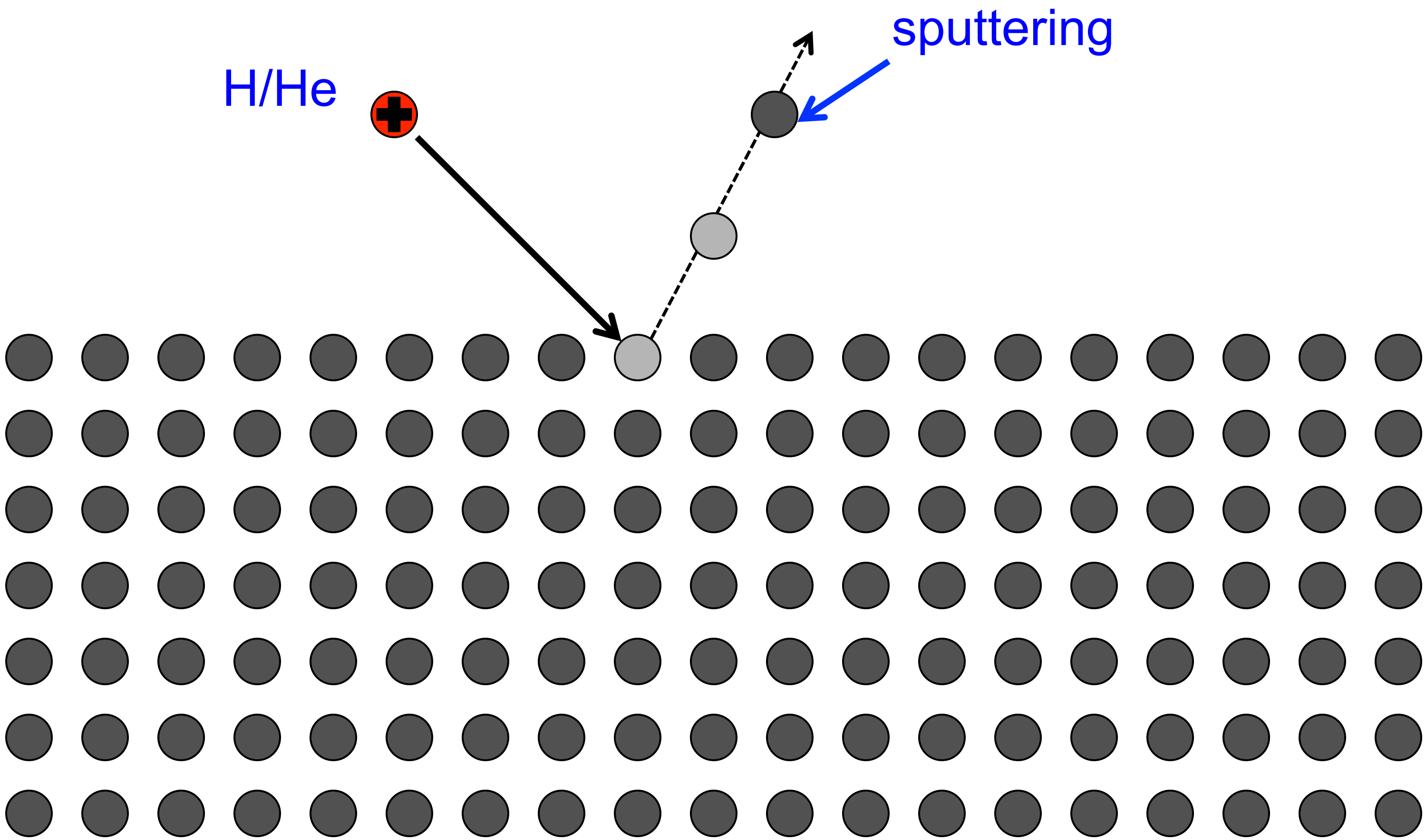

Hydrogen transport (con-ed)

- “Realistic” picture of PMI and wall processes

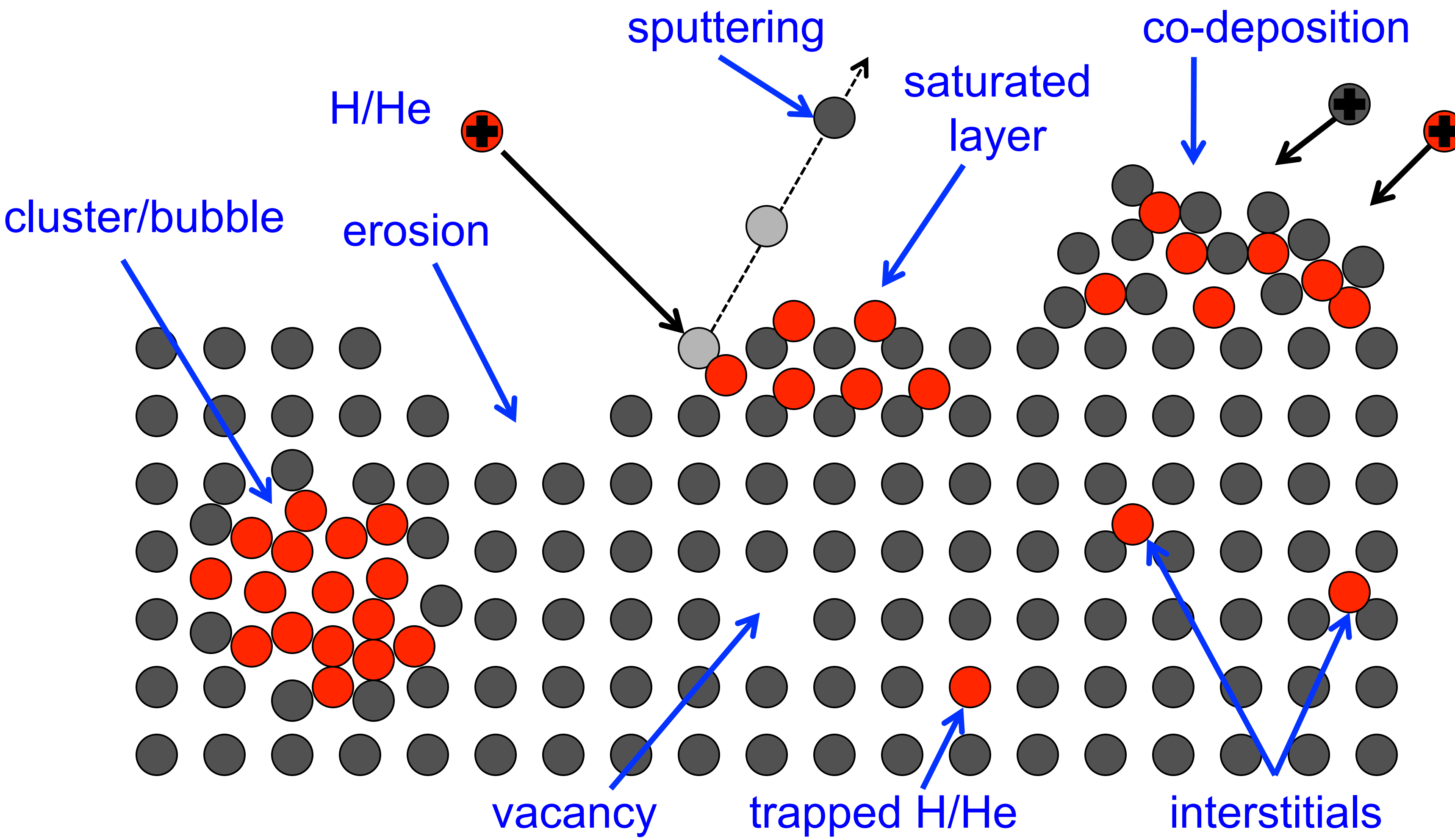

Hydrogen transport (con-ed)

- Effective potential energy for over-damped dynamics of H in solids (Tungsten, not in scale)

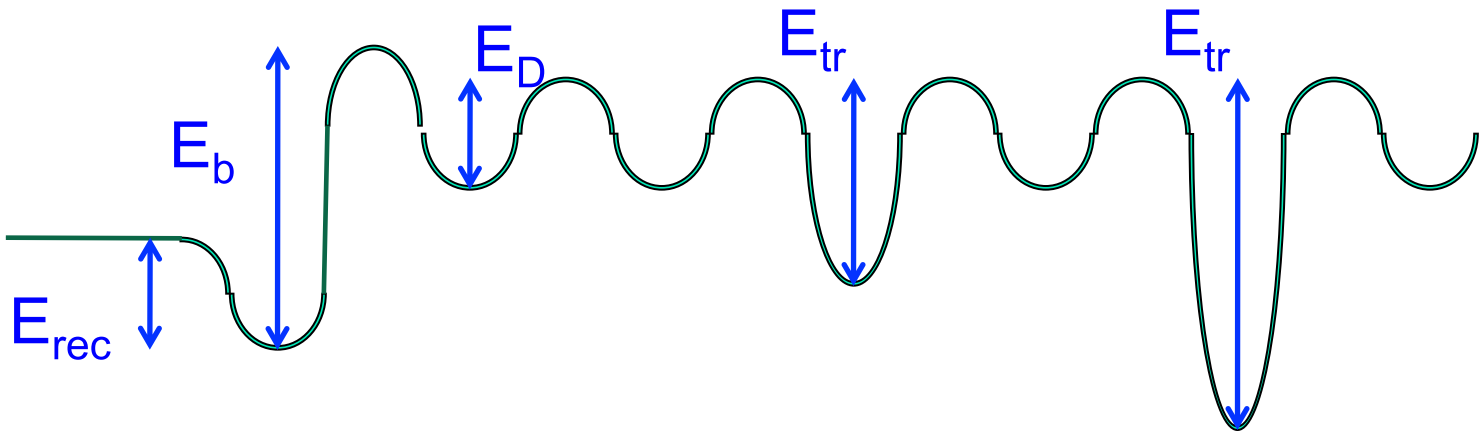

E_D~ 0.4 eV; E_{rec}~ 1 eV; $E_{tr} \geq$ 1 eV; E_b~2 eV

- Traps are caused by lattice imperfections, impurities, grain boundaries, etc.

Hydrogen transport (con-ed)

- Transport of H in solids is often separated on the diffusion of “free” and de-trapping of trapped H

thermal diffusion of “free” H

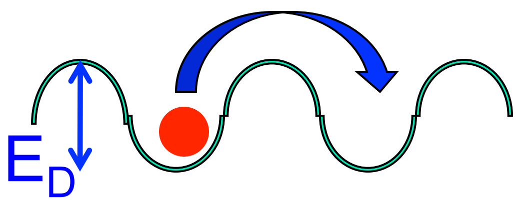

$$D = D_0 \exp(-E_D / T)$$

$$D_0 \sim 10^{-3} cm^2 / s$$

de-trapping of “trapped” H due to thermal fluctuations

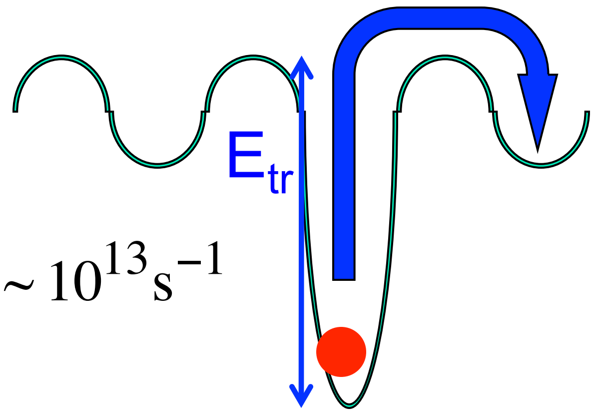

$$\nu_0 \sim 10^{13} s^{-1}$$

$$\nu_{dt} = \nu_0 \exp(-E_{tr} / T)$$

- We notice that trapping of H in C and Be is mainly caused by rather strong chemical bonds (C-H and Be-H)
  - This, in particular, explains a strong retention of H in C

Hydrogen transport (con-ed)

- While He freely leaves the surface of the solids, H (but not H_2!) is usually strongly trapped at the surface (recall potential curves!)
- Therefore, H diffuses on the surface until it “finds” another H to recombine into molecule H_2 and leave the surface
- As a result, the flux of H thermal desorption, Γ_{des} , from the surface is

$$\Gamma_{des} = [H]_s^2 K_{rec} \qquad K_{rec} = K_0^{rec} \exp(-2E_{rec}/T) \qquad K_0^{rec} \sim 10^{-3} cm^2/s$$

- However, MD simulations (Krstic, 2007) show that H outgassing from supersaturated layers occurs due to plasma ion induced desorption!

Hydrogen transport (con-ed)

- H transport in solids is often described with reaction-diffusion equations including “free” and trapped H

$$\frac{\partial n_f}{\partial t} = D_f \frac{\partial^2 n_f}{\partial x^2} - \sum_i K_{tr}^i \left(N_{tr}^i - n_{tr}^i\right) n_f + \sum_i \nu_{dtr}^i n_{tr}^i$$

$$\frac{\partial n_{tr}^i}{\partial t} = K_{tr}^i \left(N_{tr}^i - n_{tr}^i\right) n_f - \nu_{dtr}^i n_{tr}^i$$

- Even though these equations look rather simple, in practice they can describe a wide class of diffusion processes, ranging from a standard linear diffusion to nonlinear and fractional diffusion processes

Hydrogen transport (con-ed)

- For example, for a large number of different traps, they can be boiled down to fractional diffusion (Krasheninnikov, 2014), which can naturally explain power-law time dependence of long-term H outgassing $\Gamma \sim t^{-0.7}$ observed on JET and TS

$$\frac{\partial^{\alpha} n_H}{\partial t^{\alpha}} = D_{eff} \frac{\partial^2 n_H}{\partial x^2}$$

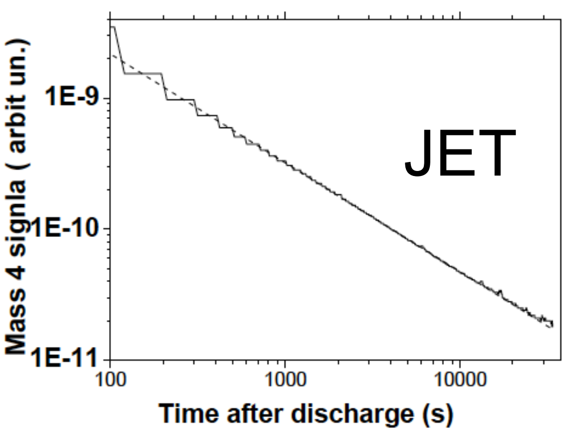

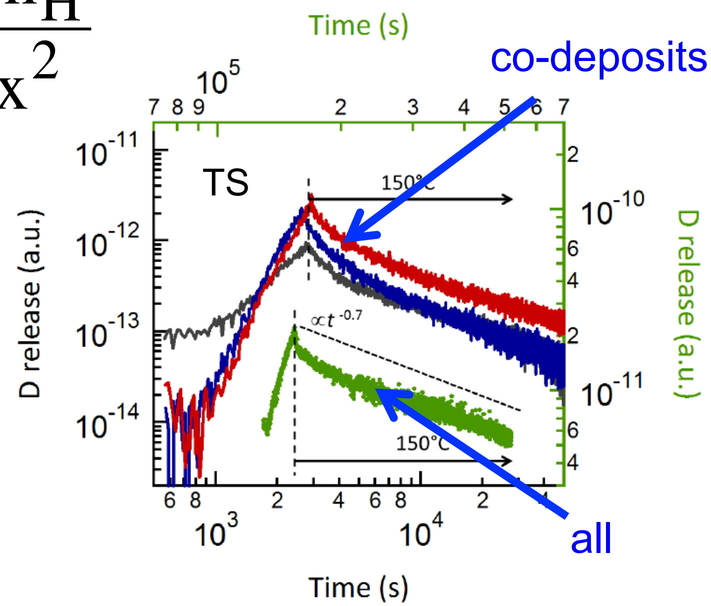

Phillips, 2013

Pégourié, 2013

Radiation transport

- Radiation transport plays important role in both normal operational regimes (e.g. divertor detachment) and abnormal events (e.g. large ELMs, disruptions)

$$\frac{4\pi c}{\hbar\omega}\vec{\Omega}\cdot\nabla I_\omega = -a_\omega I_\omega\left(B_0 N_0 - B_* N_*\right) + a_\omega N_* A$$

$$\frac{\partial N_*}{\partial t} = \nu_{exit} N_0 - \nu_{dexit} N_* - A N_* + \left(B_0 N_0 - B_* N_*\right)\frac{\int a_\omega I_\omega d\omega d\vec{\Omega}}{4\pi}$$

$I_\omega \equiv I_\omega(\vec{r},\vec{\Omega})$ -radiation intensity $\quad$ $a_\omega(\vec{r},\omega)$ -line shape

N_0 and N_* are the densities on background and excited states

A and $B_{(\dots)}$ are the Einstein coefficients

Radiation transport (con-ed)

- Line shape is rather sharp and is determined by many different processes including Doppler broadening, micro-electric fields, etc.
- This results in the fact that for the most interesting for different applications regimes of strongly trapped radiation

$$La_{\omega}(\vec{r},\omega_0)B_0N_0(\hbar\omega_0/4\pi c) >> 1$$

the main transport of radiation occurs at the wings of the line

- In practice, radiation transport can only be treated numerically
- Today, there are a few codes dealing with radiation transport for different fusion applications: EIRENE (Reiter), CRETYN (Scott), FOREV (Pestchanyi), CRAMD (Pigarov), …

Synergistic effects:
Dynamic plasma-wall interactions during ELMs

- During large type-I ELMs significant amount (up to ~30%) of pedestal plasma density is expelled from the core in a very short time (~1 ms)

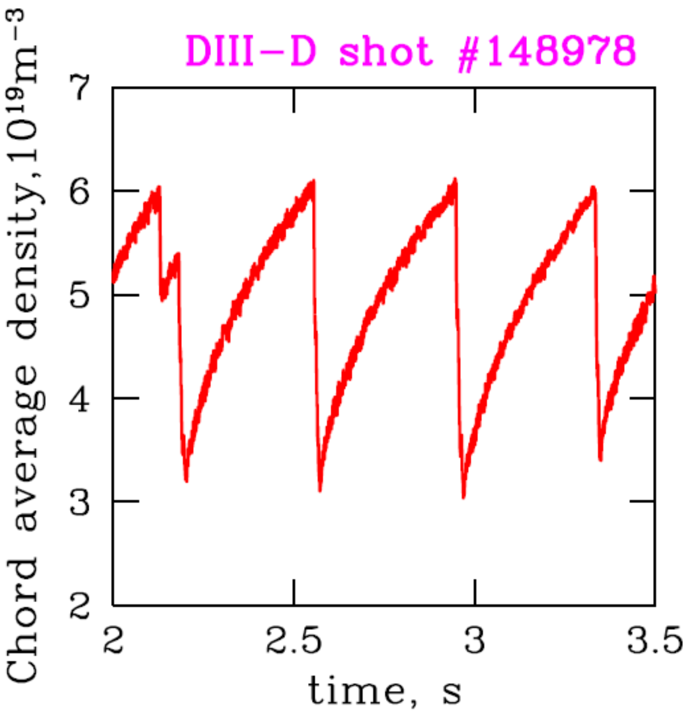

- Pedestal particle loss: $\sim 3\times10^{20}$ D
- Initial inventory in SOL+Divertors: $\sim 4\times10^{19}$ D
- After the ELM, pedestal inventory is recovering gradually during ~100÷400 ms
- NBI fueling, puffing/pumping are small!

Where are the particles expelled by ELM go to?

Where the particles are coming from to re-heal pedestal?

There are only two options:

i) Expelled particles reside in SOL and divertors

ii) Expelled particles are absorbed by the wall

Dynamic plasma-wall interactions (con-ed)

- To address this issue we use the UEDGE-MB code (Pigarov, 2011) coupled to the model describing plasma-wall particle exchange and the wall heat balance

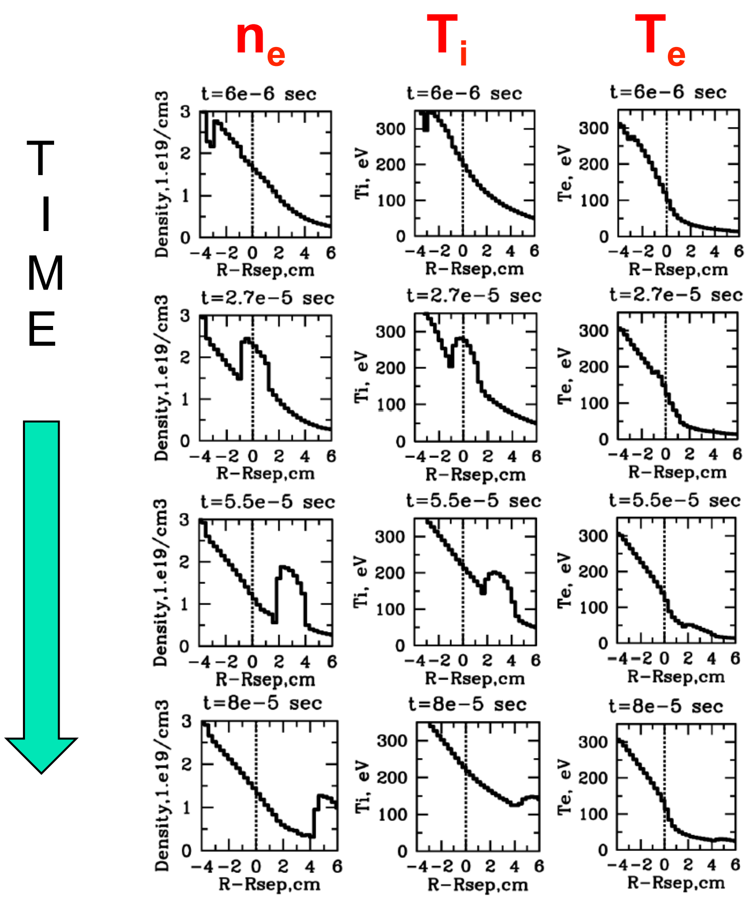

- UEDGE-MB is capable to model temporal evolution of plasma density, ion and electron temperature, as well as plasma-wall interactions during ELM event

Dynamic plasma-wall interactions (con-ed)

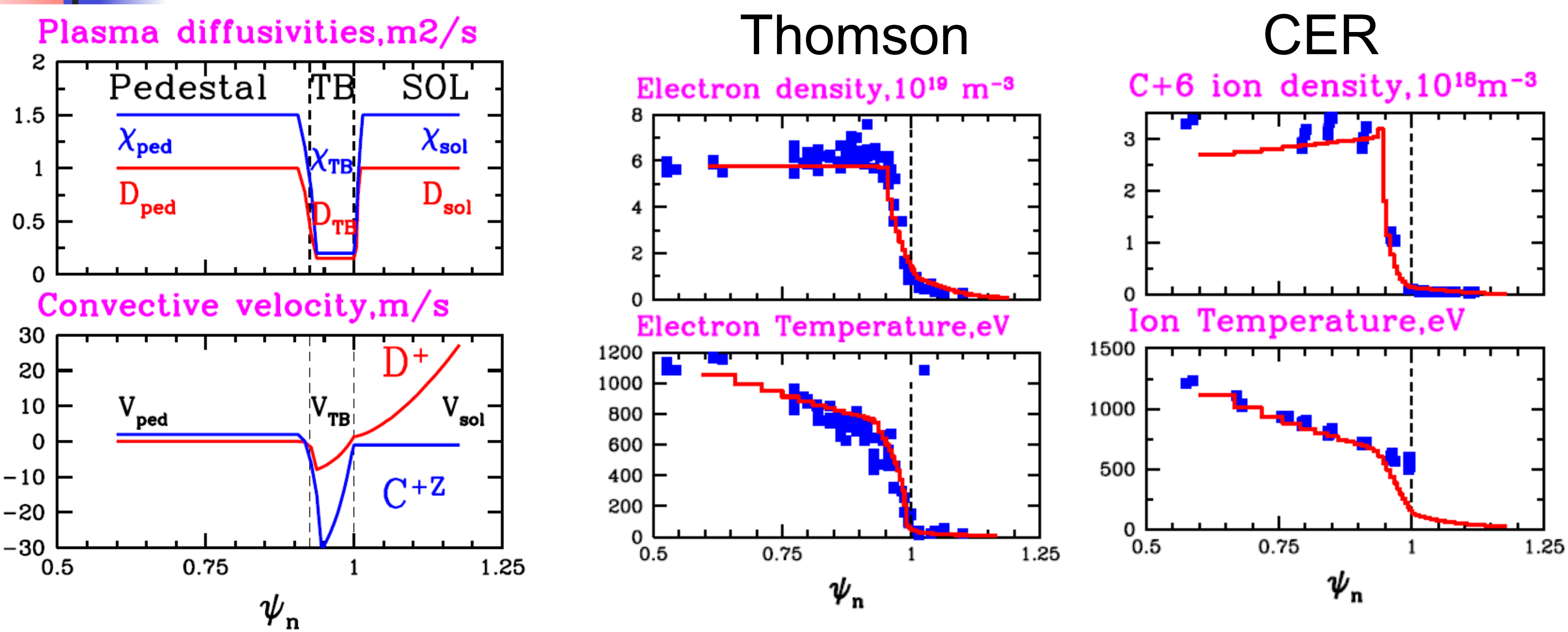

- Radial profiles of anomalous D_{perp}, χ_{perp} and V_{perp} exhibit the transport barrier
- Profiles of transport coefficients are adjusted to match experimental plasma data over the sequence of ELMs
- During the ELMs, the values of local D_{perp}, χ_{perp} and V_{perp} change to the higher values following the Macro-blob movement

Dynamic plasma-wall interactions (con-ed)

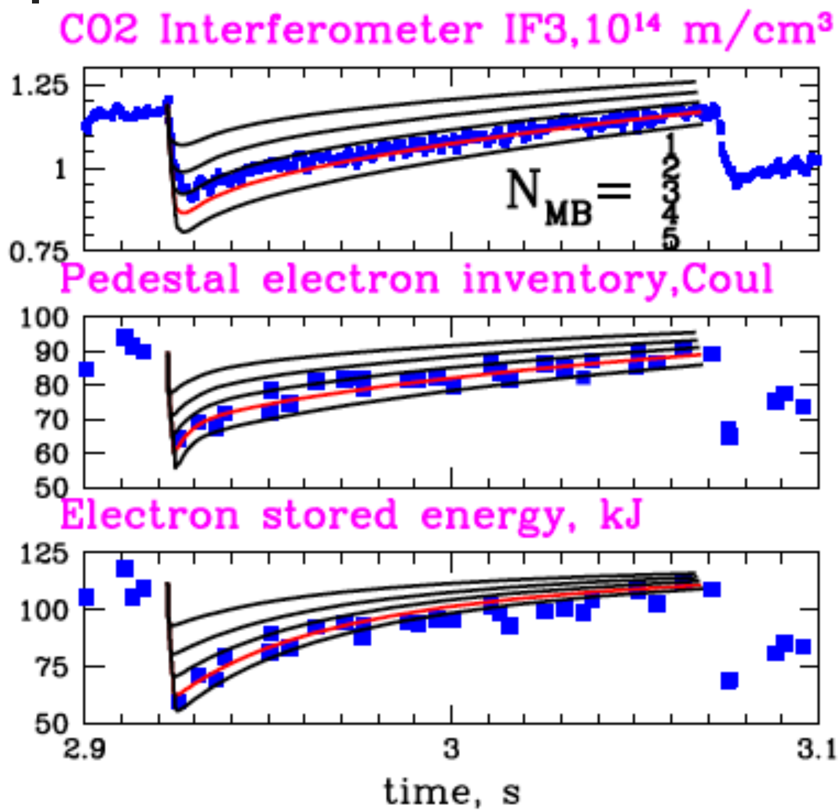

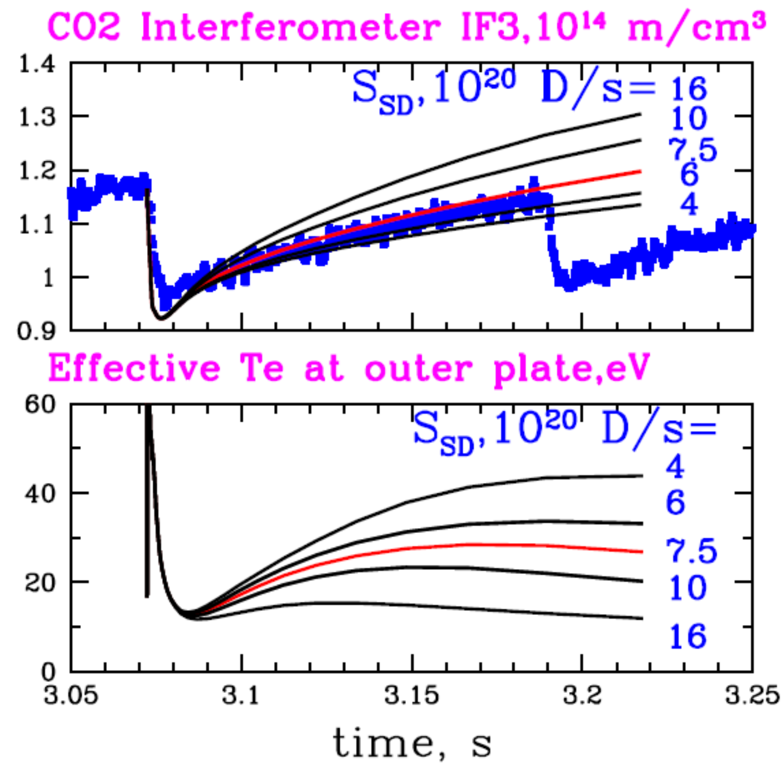

- We find the number of Macro-blobs in our ELM modeling by matching pedestal particle and energy losses in ELM
- We determine the wall parameters in our model by matching pedestal recovery dynamics

Dynamic plasma-wall interactions (con-ed)

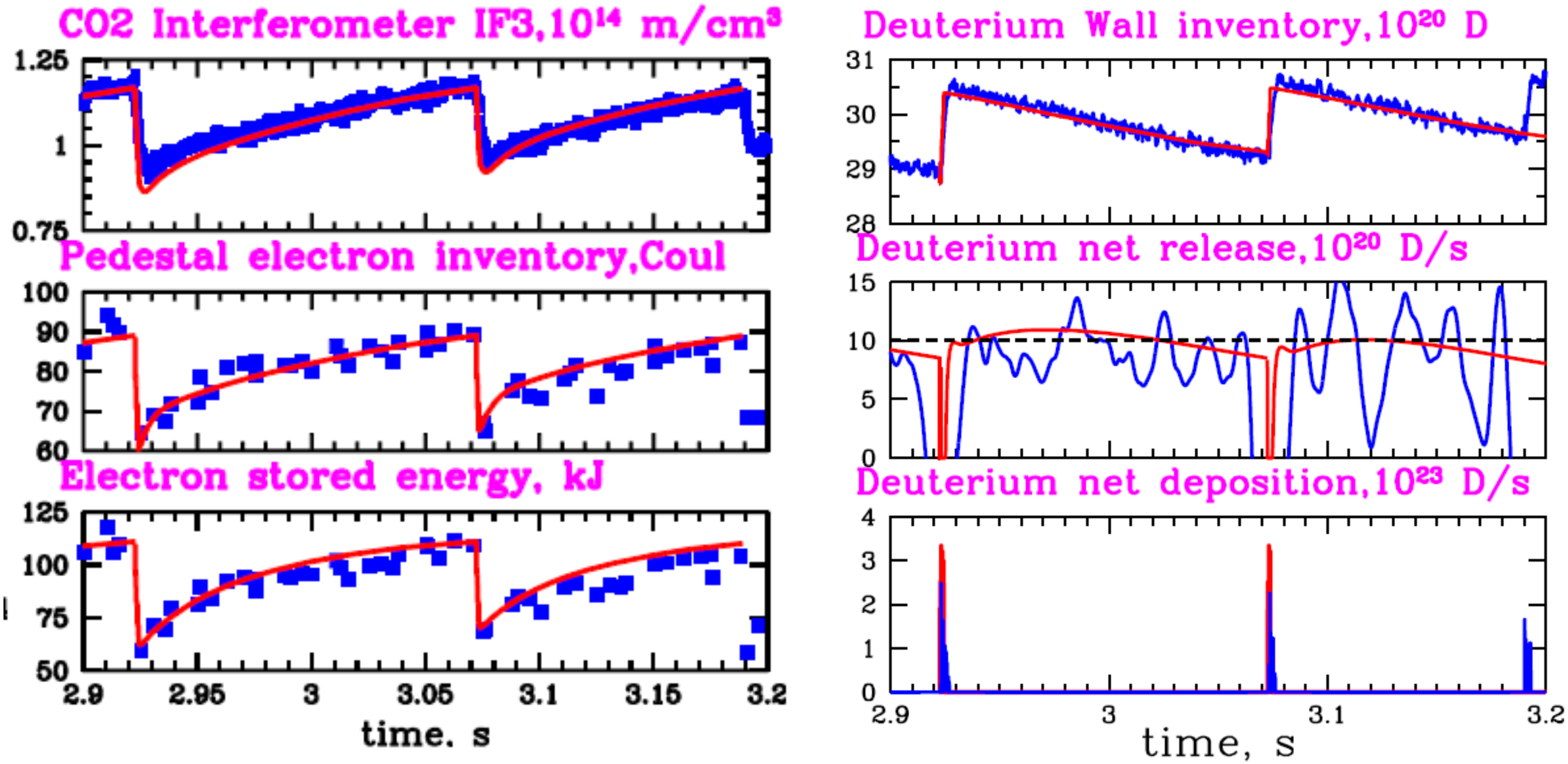

- As a result, we are able to obtain a good agreement with experimental data on a few "real" consecutive ELMs in both plasma parameter and particle inventory variations

Dynamic plasma-wall interactions (con-ed)

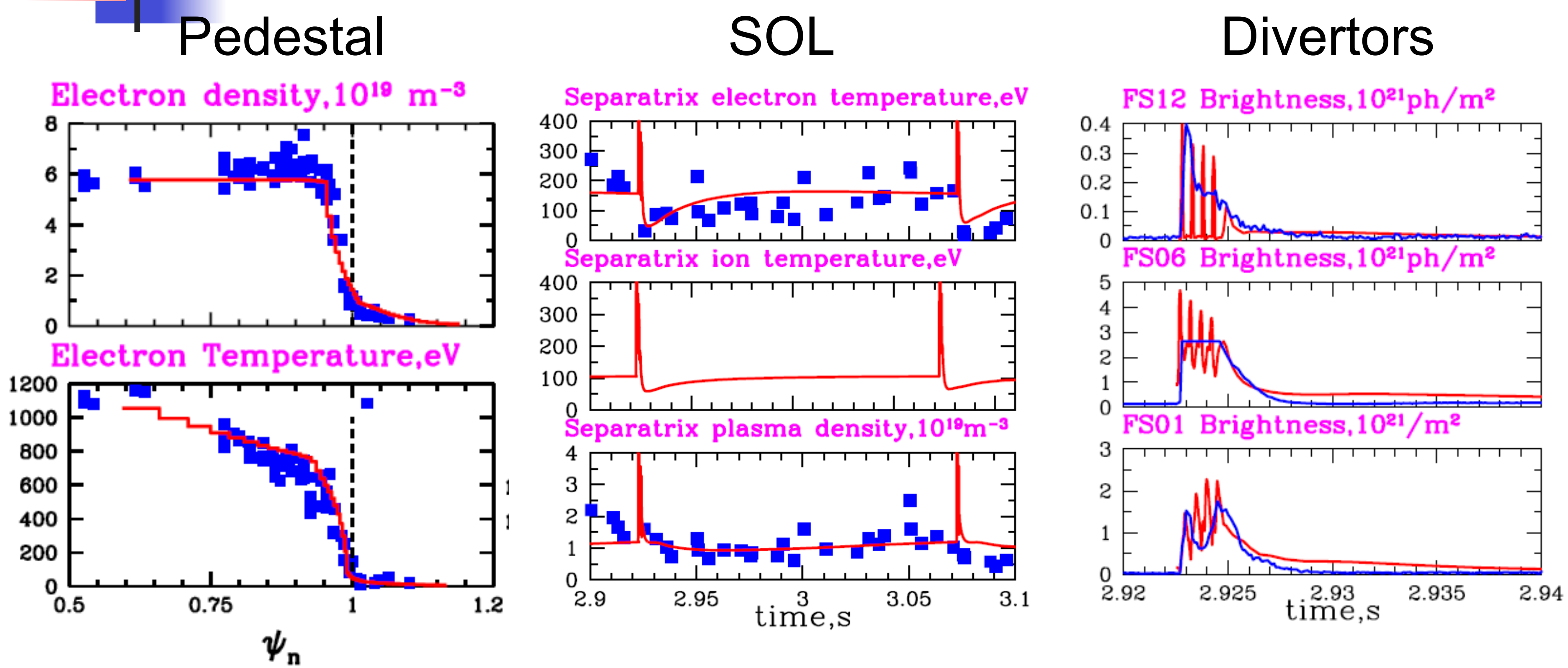

- In UEDGE-MB modeling, we use experimental data on plasma parameters in the pedestal, SOL, and divertors

Dynamic plasma-wall interactions (con-ed)

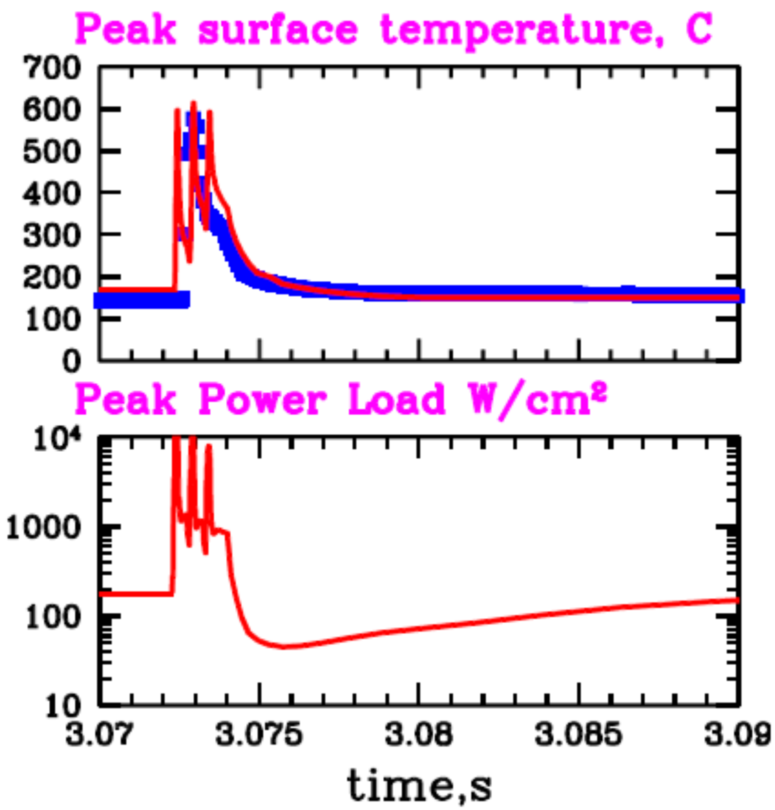

- Calculated peak power loads on divertor plates are huge ~100 MW/m^2 during ELM/surface interaction, raising the peak surface temperature up to 600 C.
- After the ELM, onset of transport barrier results in a very small heat fluxes ~0.3MW/m^2, so that the surface temperature quickly drops to 200 C as it was before the ELM
- Divertor plasma is transiently partially detached. Recovery time is ~20 ms.

Dynamic plasma-wall interactions (con-ed)

- As a result of our DIII-D simulations, we find:
  - the figure of merit for ELM-wall interactions is $\eta = \Delta N_{ped} / N_{SOL+div}$
  - for large ELMs, $\eta \approx 4$:
    - majority of particles expelled from the pedestal are absorbed by the wall
    - pedestal re-healing is determined by wall outgassing processes, which, therefore, control ELM frequency
    - stimulated desorption dominates in outgassing from the wall
  - for "small" ELMs, $\eta \approx 2$:
    - majority of particles expelled from the pedestal are reside in SOL and divertors
    - pedestal re-healing is determined by plasma and neutral gas transport processes in SOL and divertors, which, therefore, control ELM frequency

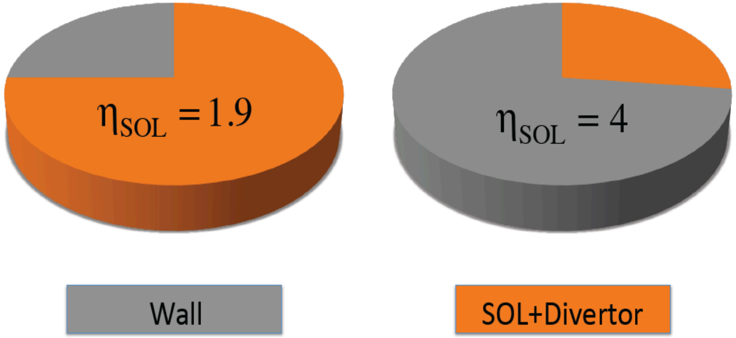

Dynamic plasma-wall interactions (con-ed)

- Outlook:
  - ITER metal wall can behave differently than carbon wall in DIII-D
    - This already have seen on JET ILW
  - High target temperature in ITER can activate thermal desorption of captured Hydrogen with potential threat of thermal instability resulting in massive ejection of gas from the wall into plasma (already observed on JT-60)

Synergistic effects: Vapor shielding

- Vapor shielding effects are clearly observed in experiments on plasma gun MK-200 simulating the interactions of large plasma heat fluxes with material
  - It was shown in particular, that the energy reaching the wall is limited by some maximum value $\hat{E}_{max}$, which can be significantly smaller than total energy $\hat{E}_0$ delivered by plasma
- Interestingly, $\hat{E}_{max}$ appears to be virtually the same for both CFC and W wall despite large difference in radiative capabilities of C and W

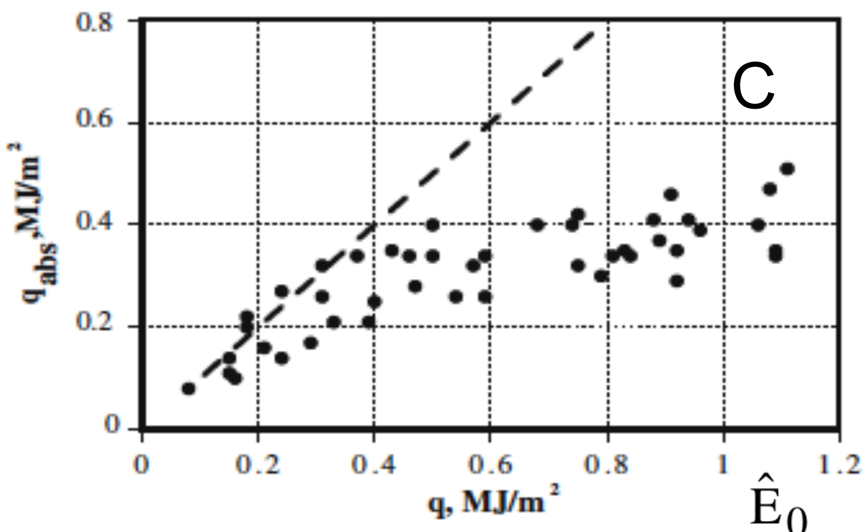

Safronov, 2008

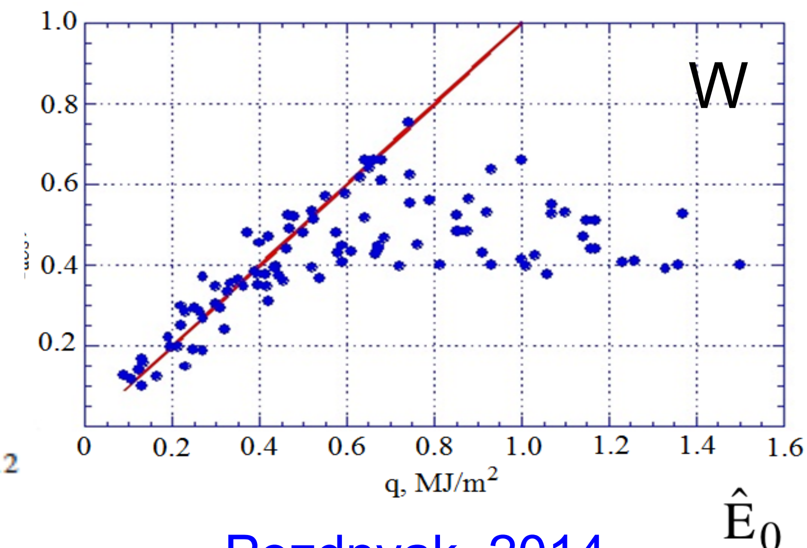

Pozdnyak, 2014

Vapor shielding (con-ed)

- To shade the light on these curies results let us consider a simple model and estimate $\hat{E}_{max}$ under assumption of the "perfect" shielding condition where we will assume that:
  - the radiation loss from ablation cloud is proportional to the total amount of evaporated material and
  - all radiation goes in the direction away from the target.

$$q_t(t) = q_0 - \dot{E}_{rad} \int_0^t j_v(t')dt' \qquad j_v(t) = j_0 \exp\{-E_{ev} / T_s(t)\}$$

$$\frac{\partial T}{\partial t} = \alpha \frac{\partial^2 T}{\partial x^2} \qquad -\kappa \left.\frac{\partial T}{\partial x}\right|_{x=0} = q_t(t)$$

- For $E_{ev} >> T_s(t)$ the most of evaporation of the target occurs during small time interval, Δt, around the time $t \sim t_* >> \Delta t$ where $q_t(t_*) \approx 0$
- For $t \,\tilde{<}\, t_*$ one can neglect shielding effects and take $q_t(t) = q_0$, which gives:

$$T_s(t) = q_0 \sqrt{4\alpha t / \pi \kappa^2}$$

Vapor shielding (con-ed)

- Then from $q_t(t_*) \approx 0$ we find:

$$t_* = \left(\frac{E_{ev}\kappa}{q_0 \Lambda}\right)^2 \frac{\pi}{4\alpha} \qquad \text{where} \qquad \Lambda = \ell n\left\{\frac{2 j_0 \dot{E}_{rad}}{E_{ev}\kappa} t_*^{3/2} \sqrt{\frac{\alpha}{\pi}}\right\} \approx 10 \div 20$$

$$\hat{E}_{max} \approx q_0 t_* \approx \left(\frac{E_{ev}\kappa}{\Lambda}\right)^2 \frac{\pi}{4\alpha q_0}$$

- We notice that $\hat{E}_{max}$ only weakly (logarithmically) depends on such "ill defined" parameter as $\dot{E}_{rad}$ and for both C and W, in agreement with experimental data, we have

$$\hat{E}_{max} \approx 0.4 \text{ MJ}/\text{m}^2$$

Vapor shielding (con-ed)

- Now we go back and examine how sensitive our estimate $\hat{E}_{max}$ with respect to the shielding model is
- As one can see, there are only two important points determine $\hat{E}_{max}$:
  - ablated material shields the surface from plasma heat flux, and
  - intense ablation, causing shielding effect, occurs in relatively short time
- Under these assumptions we find our estimate
- Therefore, the details of the processes going on in the ablation cloud and resulting in the shielding of plasma heat flux become not important for the estimation of $\hat{E}_{max}$ and cannot serve as a figure of merit for the verification of the codes

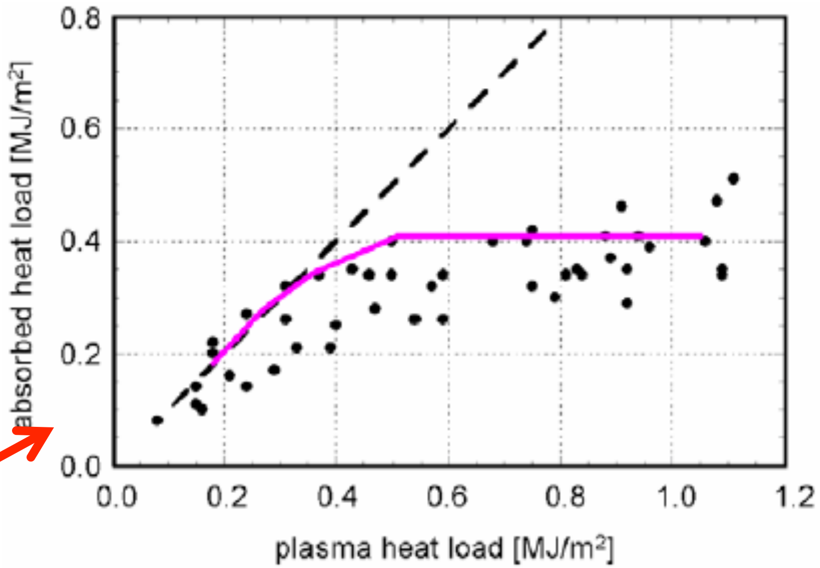

Pestchanyi, 2009

Synergistic effects: Secondary electron emission

- Secondary and thermionic electron emission from the surface contacting with plasma can significantly alter heat flux from plasma (Hobbs, 1967), result in the formation of "hot spots" (Tokar',1992), and even drive relaxation oscillations in plasma (Sydorenko, 2009)
- Usually, in theoretical studies of the effects of secondary electron emission it is assumed that electrons impinging on the surface have Maxwellian distribution function
- In this case the averaged SEE coefficient, $\delta = j_{se} / j_e$, depends only on T_e and is not altered by the variation of the floating potential φ_W
- However, in practice electron distribution function impinging on the target in the SOL of fusion devices has very pronounced cut-off of the tail due to both relatively week Coulomb collisions of tail electrons and absorption of fast electrons by the surface
- As a result, we have more interesting situation with the magnitude of δ

Secondary electron emission (con-ed)

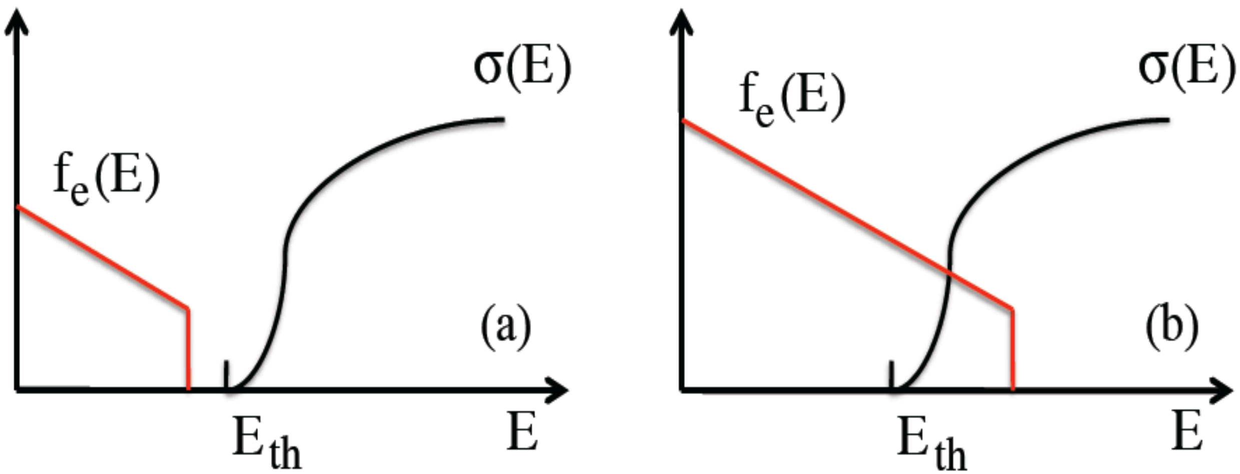

Dependence of primary electron distribution function and SEE coefficient for $E_{cut} - e\varphi_w$ smaller (a) and larger (b) than E_{th}

- Thus, we see that in this case δ depends on φ_w but, on the other hand δ affects the magnitude of floating potential φ_w
- Moreover, reduction of φ_w results in increasing energy of primary electrons coming to the surface, which may lead to the increase of δ and further decrease in φ_w

Secondary electron emission (con-ed)

- Analysis of this situation (Lee, 2014) shows that the solution of coupled plasma-wall system as the function of dimensionless parameter E_{cut}/E_{th} can bifurcate from virtually no- to large impact of the SEE effects

- In particular, the heat flux to the surface as a function of the ratio E_{cut}/E_{th} has the S-like dependence
- Applying this result to the heat transport in the SOL plasma we find that it can cause two-slope radial profile of effective electron temperature in the SOL plasma, which, actually, often seen in experiments

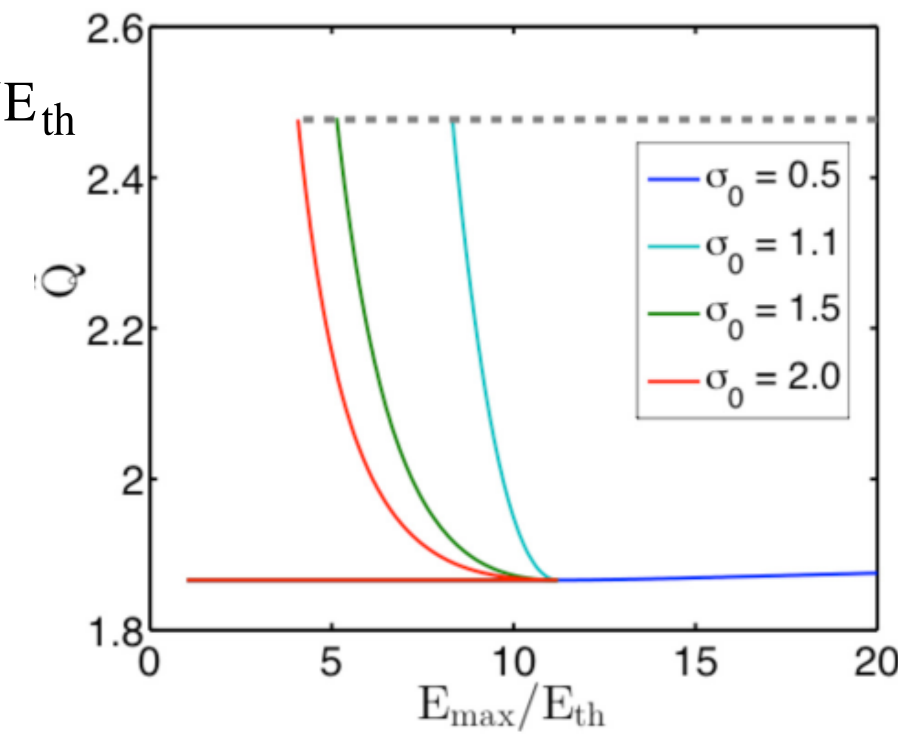

Conclusions

- There is significant amount of experimental data clearly demonstrating the synergistic effects in plasma-wall interactions in magnetic fusion devices
- Here we just highlighted some of these effects
  - We find that in infrequent giant ELMs the particles expelled from the pedestal during the ELM are dynamically retained in the wall
  - Pedestal density recovery and, therefore, ELM period, are largely controlled by the wall outgassing porcesses in the case of large ELMs and by the plasma and neutral gas transport processes in the SOL and divertor transport in the case of small ELMs
  - The situation might be different in the long pulse high power discharges in ITER, where the metallic wall will be strongly heated and thermal desorption can dominate
  - Amount of energy absorbed by the target has a week dependence on the details of the shielding processes and, therefore, cannot be the figure merit for the verification of different shielding models
  - We show that non-Maxwellian features of the electron distribution function in the SOL can cause the bifurcation of the heat flux to the target related to the effects of secondary electron emission

Acknowledgements

This work was supported by the
USDoE Grants # DE-FG02-04ER54739
and DE-SC0008660 at UCSD

Thank you


2015 © Юрий Югансон / yuhanson . livejournal . com


Виртуальная Выкса | wyksa.ru